Supplementary information

Image analysis from TEM and AFM micrographs

The size, shape and morphology of the larger particles found on the TEM and AFM-micrographs were analysed using image analysis computer software for electron microscopy (Digital Micrograph, Gatan Inc.). Particles were selected that exceeded a certain threshold in terms of thickness and electron density (for TEM) and particle height (for AFM). Each particle was thereafter automatically analysed for length and breadth (i.e., maximum and minimum diameter), projected area, perimeter and equivalent circular diameter (Table S1). From those basic parameters, for each particle the shape parameters 'roundness' and 'solidity' were calculated, according to equations 1 and 2.

$$roundness = \frac{4A}{\pi \times L^2} \qquad (1)$$

$$solidity = \frac{A}{A_C} \qquad (2)$$

where L is the particle length, A is the projected area and A_C is the convex area, i.e., the area of a convex curve connecting the outer limits of the particle. Roundness thus describes how much the shape of the particle projected area resembles a circle, with a value of unity being a perfect circle and a lower value showing that the shape deviates from a circle. Solidity describes how concave or 'entangled' the shape of the particle projected area is, with a value of unity showing a completely convex shape and lower values showing higher concavity, e.g., more entanglement.

In addition, the fractal dimensions were calculated in the first dimension (D_1), second dimension (D_2) and third dimension (D_3) using a simplified approach described by Lee and Kramer (2004), using equations 3, 4 and 5:

$$D_1 = \frac{\log(P)}{\log(L)} \qquad (3)$$

$$D_2 = \frac{\log(A)}{\log(L)} \qquad (4)$$

$$D_3 = 1.391 + 0.01 \times e^{2.164 \times D_2} \qquad (5)$$

where P is the perimeter of the particle projected area.

Table S1. Size and shape parameters and fractal dimensions of particles measured on TEM-micrographs (median values ± upper quartile/lower quartile).

Site	Particle number	Length (nm)	Breadth (nm)	Circular diameter (nm)	Roundness (nm)	Solidity (nm)	D1	D2	D3
A	10	700 ± 1300/560	400 ± 700/340	600 ± 1020/500	0.3 ± 0.33/0.24	0.6 ± 0.64/0.48	1.27 ± 1.291/1.260	1.77 ± 1.797/1.754	1.86 ± 1.880/1.837
B	10	200 ± 360/60	100 ± 150/30	200 ± 260/50	0.4 ± 0.45/0.24	0.6 ± 0.80/0.57	1.34 ± 1.366/1.305	1.74 ± 1.747/1.715	1.83 ± 1.830/1.800
C	14	800 ± 1360/540	400 ± 650/330	600 ± 1080/480	0.3 ± 0.45/0.16	0.5 ± 0.60/0.38	1.33 ± 1.351/1.298	1.74 ± 1.829/1.722	1.83 ± 1.914/1.806
D	11	900 ± 1760/290	600 ± 810/180	800 ± 1370/240	0.3 ± 0.35/0.26	0.5 ± 0.64/0.40	1.31 ± 1.330/1.281	1.78 ± 1.809/1.752	1.86 ± 1.892/1.835

Table S2. Sizes of particles measured on AFM-micrographs (median values ± upper quartile/lower quartile).

Site	Particle numbers	Particle height (nm)	Equivalent spherical volume (nm^3)
A	226	4 ± 6.6/2.4	50 ± 150/7
B	201	3 ± 6.1/1.9	20 ± 120/3
C	231	6 ± 9.1/4.2	110 ± 400/40
D	209	4 ± 5.5/2.5	20 ± 87/9

Table S3. Fractal dimension of aggregates, measured on AFM-micrographs (median values ± upper quartile/lower quartile).

Site	Particle numbers	D1	D2	D3
A	29	1.4 ± 1.49/1.39	1.7 ± 1.77/1.67	1.83 ± 1.85/1.76
B	30	1.47 ± 1.527/1.444	1.7 ± 1.78/1.63	1.8 ± 1.86/1.73
C	53	1.41 ± 1.442/1.366	1.7 ± 1.80/1.68	1.8 ± 1.89/1.77
D	11	1.50 ± 1.522/1.440	1.7 ± 1.73/1.62	1.77 ± 1.81/1.73

Figure S1

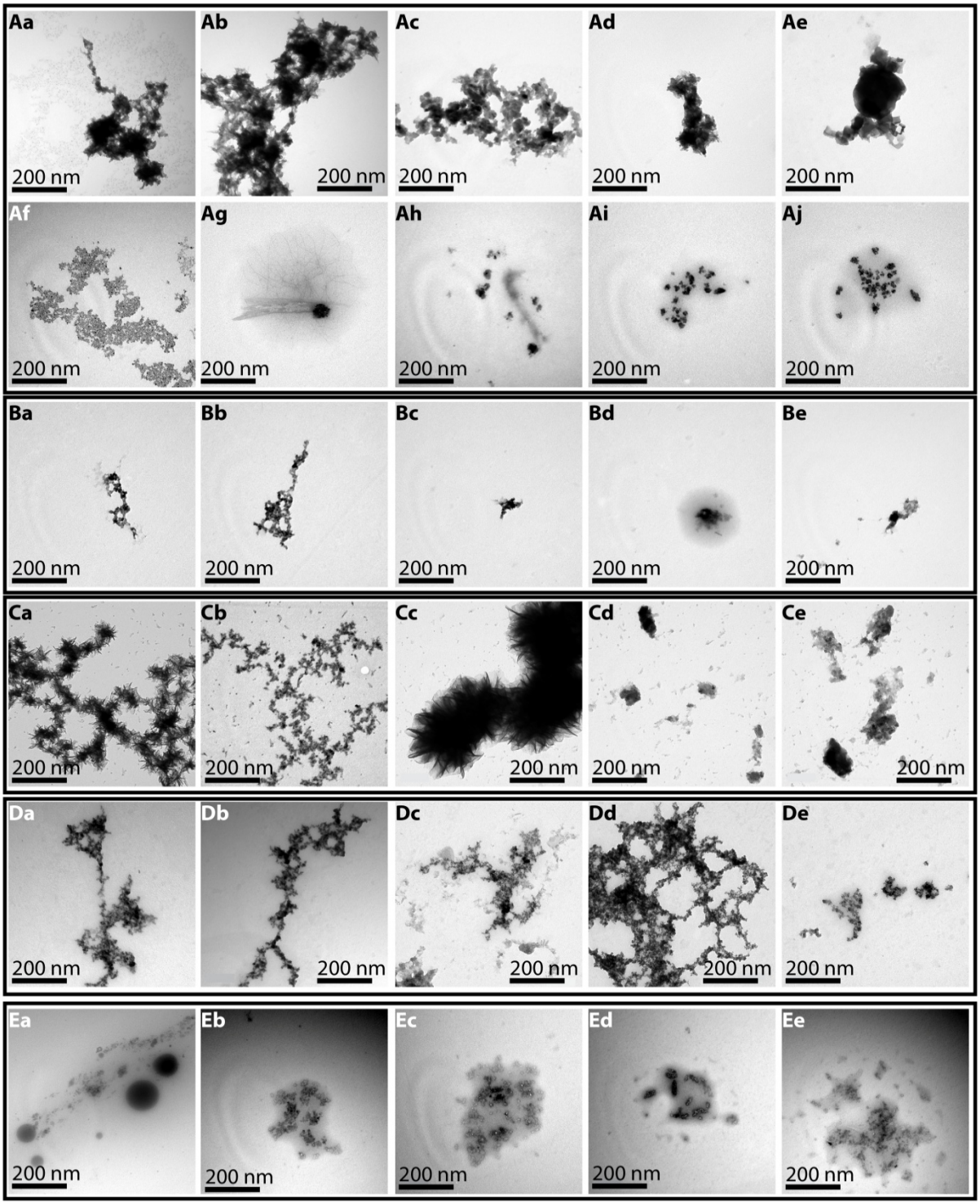
Aa
Ab
Ac
Ad
Ae
Af
Ag
Ah
Ai
Aj
Ba
Bb
Bc
Bd
Be
Ca
Cb
Cc
Cd
Ce
Da
Db
Dc
Dd
De
Ea
Eb
Ec
Ed
Ee
200 nm

Figure S2

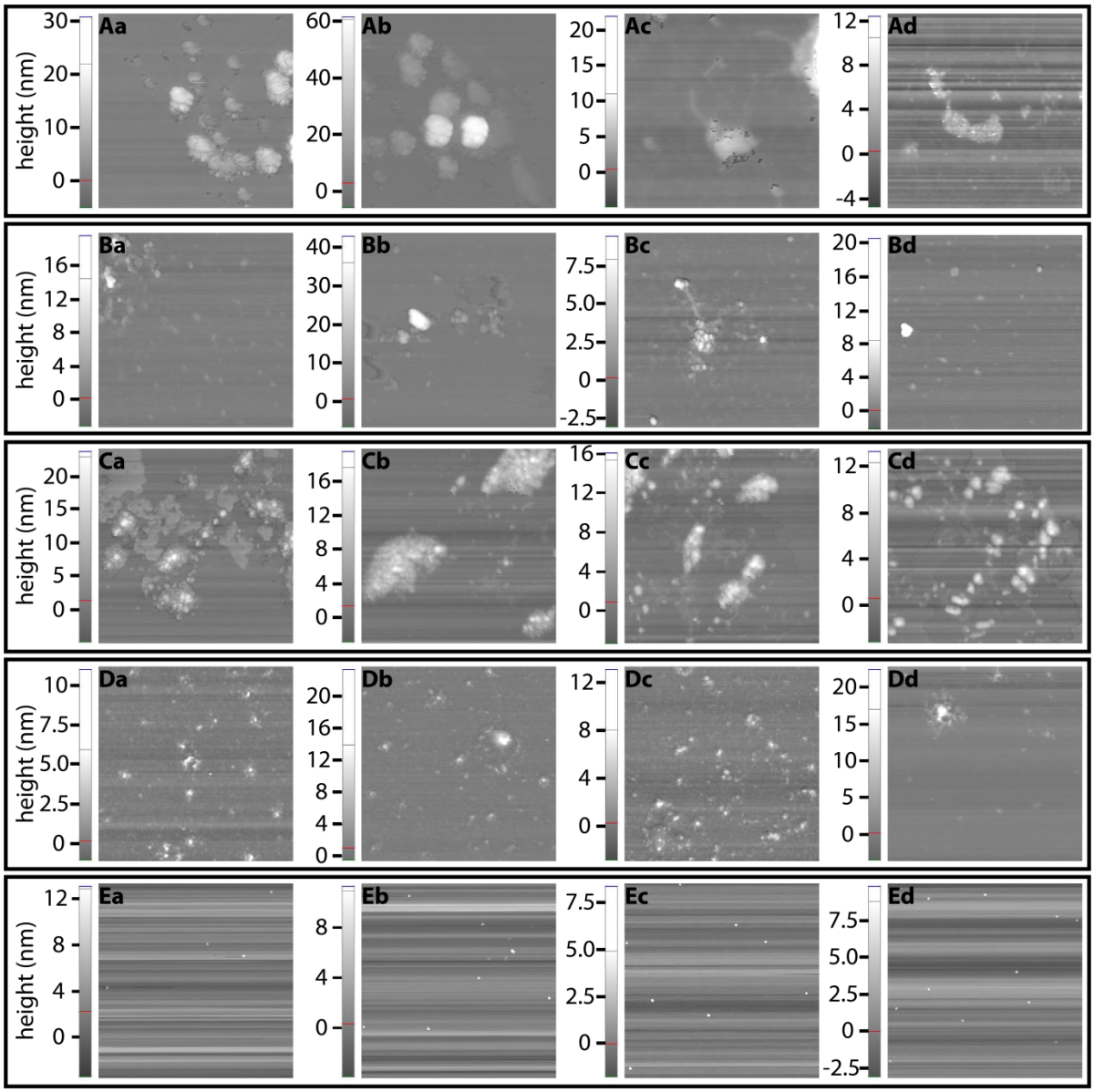

Fig S1 TEM-micrographs from the sampling sites with low-pH (Aa-Aj), mid-pH (Ba-Be), the control site (Ca-Ce), extremely low-pH (Da-De) and from the hydrothermal gas captured using the aerosol nanoparticle sampler (Ea-Ee). The low-pH, mid-pH and control samples contained particles with different morphology and element-composition, e.g., typical Fe-rich colloids (shown in micrographs Aa-Ae, Aa-Bc and Ca-Cc), particles rich in Ca, Na and S (Ah-Aj, Bd-Be, presumed Ca-carbonate or salt-precipitates), particle especially rich in K (Ag, presumed plankton cell), and small particles for which EDX could only detect low levels of Ca and S (Af, presumed organic macromolecules or small iron-rich nanoparticles). The extremely low-pH sample contained colloids rich in S that were composed of smaller nanoparticles (Da-Dd) as well as more Fe-rich particles (De). The gas samples contained clusters of small particles rich in S, Ca, K, Mg, P and Si with traces of Fe and Co.

Fig S2 AFM-images from the sample sites with low-pH (Aa-Ad), mid-pH (Ba-Bd), the control site (Ca-Cd), extremely low-pH (Da-Dd) and from the hydrothermal gas captured using the aerosol nanoparticle sampler (Ea-Ed).